ISSN 2472-1972

Insights Into the Mechanism of MCT8 Oligomerization

Stefan Groeneweg,[1] Amanda van den Berge,[1] Elaine C. Lima de Souza,[1] Marcel E. Meima,[1] Robin P. Peeters,[1] and W. Edward Visser[1]

[1]*Academic Center for Thyroid Diseases, Department of Internal Medicine, Erasmus Medical Center, 3015 CN Rotterdam, the Netherlands*

ORCiD number: 0000-0001-6879-7392 (S. Groeneweg).

Mutations in the thyroid hormone transporter monocarboxylate transporter 8 (MCT8) result in MCT8 deficiency, characterized by severe intellectual and motor disability. The MCT8 protein is predicted to have 12 transmembrane domains (TMDs) and is expressed as monomers, homodimers, and homo-oligomers. This study aimed to delineate the mechanism of MCT8 oligomerization. Coimmunoprecipitation studies demonstrated that lithium dodecyl sulfate effectively disrupts MCT8 protein complexes, indicating the involvement of non-covalent interactions. Successive C-terminal truncations of the MCT8 protein altered the oligomerization pattern only if introduced in the N-terminal half of the protein (TMD1-6). The truncation at extracellular loop 1 (E206X) still allowed homodimerization, but completely abrogated homo-oligomerization, whereas both were preserved by the C231X mutant (at TMD2), suggesting that the minimally required oligomerization sites are located proximal of Cys231. However, mutant constructs lacking the intracellular N-terminus or TMD1 and 2 were still capable to form homo-oligomers. Therefore, other domains distal of Cys231 are also likely to be involved in the formation of extensive multidomain interactions. This hypothesis was supported by structural modeling. Despite multiple approaches, MCT8 oligomerization could not be fully abrogated unless a substantial part of the protein was removed, precluding detailed studies into its functional role. Together, our findings suggest that MCT8 oligomerization involves extensive noncovalent interactions between the N-terminal halves of MCT8 proteins. Most mutations identified in patients with MCT8 deficiency have only minor effects on MCT8 oligomerization and, thus, impaired oligomerization does not appear to be an important pathogenic mechanism.

Key Words: MCT8, AHDS, thyroid hormone, thyroid hormone transporter, oligomerization, dimerization

Normal brain development is highly dependent on adequate intracerebral thyroid hormone (TH) concentrations. Monocarboxylate transporter 8 (MCT8) plays a crucial role in the maintenance of TH homeostasis in the brain [1]. Mutations in the *SLC16A2* gene, encoding MCT8, result in MCT8 deficiency, also known as Allan-Herndon-Dudley syndrome (AHDS), characterized by severe intellectual and motor disability, and abnormal thyroid function tests [2, 3]. Many inactivating mutations have been reported to date, with different underlying pathogenic mechanisms [4].

Abbreviations: Abs, antibodies; AHDS, Allan-Herndon-Dudley syndrome; cDNA, complementary DNA; co-IP, coimmunoprecipitation; CRYM, human μ-crystallin; DTT, dithiothreitol; ECL, extracellular loop; GAPDH, glyceraldehyde-3-phosphate dehydrogenase; ICL, intracellular loop; IP, immunoprecipitation; LDS, lithium dodecyl sulfate; MCT8, monocarboxylate transporter 8; PAGE, polyacrylamide gel electrophoresis; SDS, sodium dodecyl sulfate; T3, 3,5,3′-triiodothyronine; T4, thyroxine; TH, thyroid hormone; TMD, transmembrane domain; WT, wild-type.

Received 27 May 2020
Accepted 12 June 2020
First Published Online 18 June 2020
Corrected and Typeset 22 July 2020

The MCT8 protein is predicted to consist of 2 nearly symmetrical parts composed of 6 transmembrane domains (TMDs), interconnected by a large intracellular loop. The C-terminus and N-terminus both are predicted to be located intracellularly [5, 6]. The MCT8 protein is expressed as a monomer, homodimer, and possibly also as a homo-oligomer, in transient and stable overexpression systems [7, 8]. Recently it has been shown that MCT8 dimers are present in a cellular context, and it was suggested that missense mutations in MCT8 differentially affect oligomerization potency [9]. Modulation of the MCT8 molecular surface by these mutations has been proposed as the mechanism accounting for this finding. Nevertheless, none of these mutations completely abrogated MCT8 oligomerization [9]. Different protein oligomerization mechanisms have been described, including the formation of covalent (eg, disulfide bonds), electrostatic (eg, ionic bonds and hydrogen bonds) or hydrophobic interactions, or mediation of monomer-monomer contacts through ions (Ca^{2+} or Mg^{2+}) or small molecules (eg, [10-16].). Conventional immunoblot studies have shown that MCT8 oligomers are at least partially resistant to the denaturing effects of the chaotropic agent sodium dodecyl sulfate (SDS) and the reducing effects of dithiothreitol (DTT), suggesting that MCT8 oligomerization is not solely mediated by (weak) noncovalent interactions or disulfide bonds [7]. Indeed, all cysteine (Cys) residues within MCT8 can be substituted by Alanine (Ala) without affecting its oligomerization [7, 17].

Despite these studies, the exact mechanism involved in MCT8 oligomerization and the domain(s) of the MCT8 protein involved in this process remain to be characterized. It is furthermore unknown whether the monomers (and dimers) detected on conventional immunoblots arise from the disruption of oligomeric complexes or solely reflect the quaternary protein organization inside the cell. Lack of this knowledge precludes further studies into the relevance of MCT8 oligomerization for transporter function. It is also unclear whether specific naturally occurring mutations in MCT8 may abrogate MCT8 oligomerization and to what extent this contributes to the pathogenicity of such mutations.

We aimed to further delineate the MCT8 oligomerization mechanism and identify the domains involved in this process. Because MCT8 is able to form homo-oligomers, we postulated that each MCT8 protein should be able to interact with at least 2 other MCT8 proteins and should therefore contain at least 2 distinct domains that are involved in the formation of monomer-monomer contacts. Our findings indeed support that MCT8 oligomerization is mediated through extensive hydrophobic and electrostatic interactions between distinct domains within the N-terminal half of the protein, composed of multiple TMDs and putative loops. Despite multiple approaches, MCT8 oligomerization could not be fully abrogated unless a substantial part of the protein was removed, preventing studies into its functional role. Thus, our studies provide novel insights on the quaternary structural organization of MCT8.

1. Materials and Methods

A. Materials

Unlabeled iodothyronines, DTT and EDTA, were obtained from Sigma-Aldrich. [^{125}I] 3,5,3′-triiodothyronine (T3) and [^{125}I] thyroxine (T4) were synthesized as previously described [18]. X-tremeGENE 9 transfection reagent was obtained from Roche Diagnostics. An overview of all commercially available primary and secondary antibodies (Abs) is provided in Supplemental Table 1 [19]. Purified polyclonal rabbit antiserum against the C-terminus of human MCT8 (designated 1306, RRID:AB_2661880 [20]), and human MCT10 (designated 1758, RRID: AB_2661879 [21]) have been described previously [22, 23].

B. Plasmids

Cloning of wild-type human MCT8 (WT MCT8) complementary DNA (cDNA) into pcDNA3, human WT MCT10 cDNA into pcDNA3, and human μ-crystallin (CRYM) into pSG5 has been

described previously [22, 23]. CRYM is a cytosolic TH-binding protein that greatly reduces the efflux of TH, thereby increasing the net cellular TH accumulation. The WT MCT8 construct used in the present studies contains the coding sequence for the short MCT8 isoform, starting at the second translational start site ($MCT8_{75\text{-}613}$). The N-terminally Flag-tagged human MCT8 (Flag-MCT8) construct was cloned into pcDNA3 after polymerase chain reaction amplification of WT MCT8 cDNA using forward primers containing the Flag-tag sequence (Supplemental Table 2) [19]. The cloning of N-terminally Myc-tagged MCT8 has been described previously [24]. We introduced the following mutations into the nontagged WT MCT8 construct using QuikChange site-directed mutagenesis (Stratagene) according to the manufacturer's protocol: E206X, C231X, R245X, F256X, Q335X, S448X, Q520X, and C546X. The locations of these mutations are indicated in Supplemental Fig. 1 [19]. N-terminally truncated MCT8 constructs were generated by substituting the native translational start

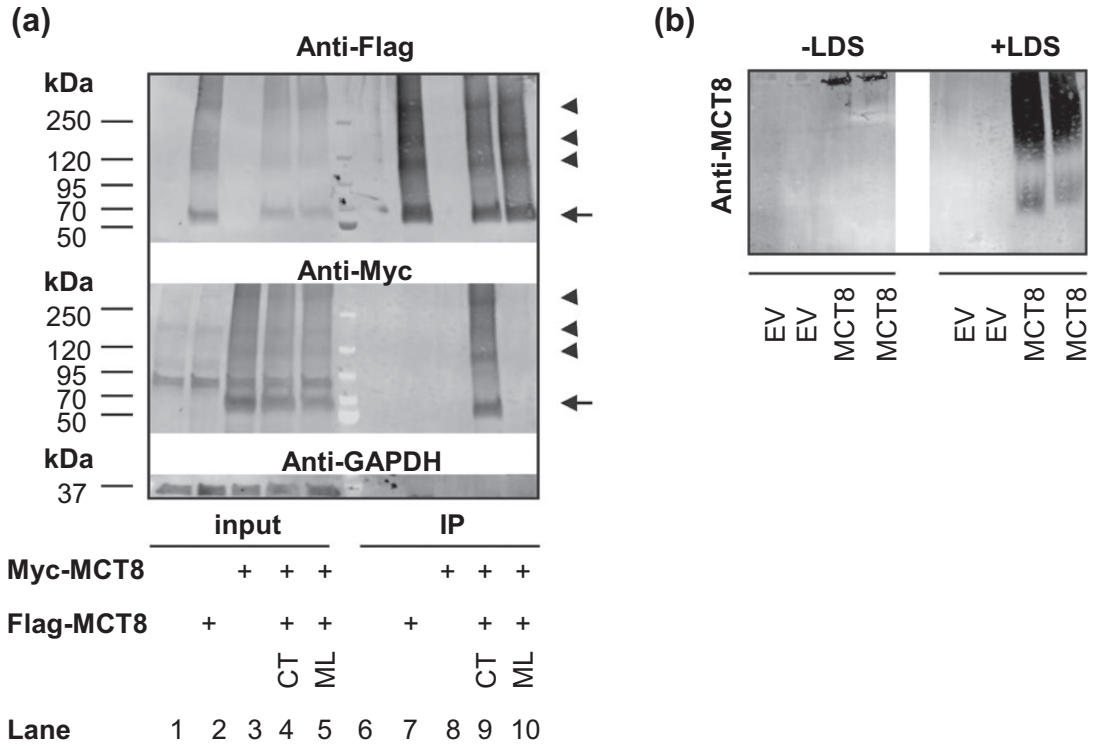

Figure 1. A, Coimmunoprecipitation studies on lysates derived from COS-1 cells transiently expressing Flag-MCT8 (lanes 2 and 7), Myc–monocarboxylate transporter 8 (MCT8) (lanes 3 and 8), or both tagged constructs (lanes 4 and 9). To exclude that the homodimerization results from an assay artifact, sonicated lysates derived from cells separately expressing Flag-MCT8 or Myc-MCT8 were mixed and incubated for 30 minutes on ice, prior to the immunoprecipitation (IP) step (lanes 5 and 10). COS-1 cells transfected with pcDNA3 empty vector (EV) were taken along as a negative control (lanes 1 and 6). Lysates were incubated in lithium dodecyl sulfate (LDS) loading buffer without dithiothreitol. The mouse monoclonal M2 Flag antibody was used for Flag-MCT8 detection, and rabbit monoclonal anti-Myc for Myc-MCT8 detection. Glyceraldehyde-3-phosphate dehydrogenase (GAPDH) was used to demonstrate the absence of nonspecific proteins in the IP sample. Note that Myc-MCT8 was detected in the IP sample only when coexpressed with Flag-MCT8 (lane 9). MCT8 monomer is indicated with an arrow and MCT8 dimer and oligomers with an arrowhead. B, Native PAGE on lysates of COS-1 cells transiently transfected with pcDNA3 empty vector (EV) or wild-type MCT8. A total of 25 µg of total lysate was either incubated in the presence of LDS-containing NuPAGE sample loading buffer at 70 °C for 10 minutes (+LDS) or kept at room temperature in native sample loading buffer (final concentrations: 31.25 mM Tris-HCl (pH 6.8), 12.5% glycerol, 0.5% bromophenol blue) in the absence of LDS (–LDS, native conditions) prior to separation under native conditions (1×PAGE buffer). MCT8 detection was performed with the N-terminal MCT8 antibody (3353) and visualized with IRDye680 goat-antirabbit secondary antibody. CT, cotransfected; EV, empty vector; ML, mixed lysates.

site by an Ala (resulting construct will be referred to as $MCT8_{M75A}$). Next, downstream translational start sites were reintroduced, resulting in the N-terminally truncated constructs $MCT8_{97-613}$ and $MCT8_{147-613}$. All used primer pairs are listed in Supplemental Table 2 [19]. Sanger sequencing was performed to confirm the presence of the introduced mutations.

To generate a construct lacking TMD1 and 2 (referred to as delTMD1/2), amino acids 170 to 234 were removed from the WT MCT8 cDNA construct using a unique EcoNI restriction site located at nucleotide position 503 to 513 and a second EcoNI site that was introduced by site-directed mutagenesis at position 697 to 707 (primers in Supplemental Table 2) [19]. After EcoNI digestion and gel purification, (QIAquick Gel Extraction Kit; Qiagen) the linear cDNA lacking nucleotides 507 to 701 was religated using T4 ligase (Roche). The deletion of C507-T701 was confirmed by DNA sequencing (Baseclear). A Flag-tagged variant of this construct was generated as described earlier.

An MCT1/8 chimera was generated by amplification of the cDNA sequence encoding the 5′UTR, translational start-site and the first 9 amino acids (covering the small intracellular N-terminal domain) of MCT1 from the pCMV-Sport6_MCT1 construct (Open Biosystems). Hind III and Nhe I restriction sites were added at the 5′ and 3′ end, respectively, using primers listed in Supplemental Table 2 [19]. A fragment of 164 base pairs ranging from C502 to C666 was next amplified from the WT MCT8 construct and an Nhe I site was added at the 5′ end (primers in Supplemental Table 2) [19]. A Bam HI restriction site was already present within the amplified fragment. Both polymerase chain reaction products were first digested with Nhe I, purified, and ligated, resulting in a chimeric MCT1/8 fragment. This fragment was further digested with Hind III and Bam HI, gel-purified, and ligated into a Hind III/Bam HI digested WT MCT8 cDNA construct. The chimeric construct was sequenced to confirm proper ligation.

C. Cell Culture and Transfection

COS-1 African green monkey kidney (CVCL_0223) and JEG-3 human choriocarcinoma (CVCL_0363) cells were obtained from ECACC (Sigma-Aldrich) and were cultured in 6- or 24-well plates (Corning) in DMEM (Dulbecco's Modified Eagle Medium)/F12 medium (Invitrogen), containing 9% heat-inactivated fetal bovine serum (Invitrogen), 2% Pen/Strep (Roche), and 100 nM sodium selenite (Sigma-Aldrich). All transient transfections were performed using X-tremeGENE 9, according to the manufacturer's protocol (Roche). We have previously shown the absence of differences in transfection efficiency between WT and mutant MCT8 constructs [25].

D. Thyroid Hormone Uptake Experiments

For TH uptake studies, COS-1 or JEG-3 cells were seeded in 6-well plates and cotransfected in duplicate at 75% confluence with indicated amount of pcDNA3 empty vector (EV) control, or indicated amount of WT or mutant MCT8 and 500 ng CRYM or pcDNA3 EV. Two days after transfection, cells were washed with incubation buffer (Dulbecco's phosphate-buffered saline containing 0.1% D-glucose and 0.1% bovine serum albumin) and subsequently incubated for 30 minutes at 37 °C in incubation buffer containing 1 nM unlabeled T3 or T4 and 5×10^5 cpm [^{125}I]T3 or [^{125}I]T4, respectively. After incubation, cells were briefly washed with incubation buffer and lysed with 0.1 M sodium hydroxide. The amount of radioactivity in the lysates was measured with a gamma counter.

E. Coimmunoprecipitation Studies

COS-1 cells cultured in 6-well plates were transfected with 500 ng of indicated constructs. Lysates were prepared 48 hours after transfection in immunoprecipitation (IP) buffer (50 mM Tris-HCl, 150 mM NaCl, 10 mM EDTA, 1% Triton-X-100) containing protease inhibitor cocktail (Roche) and incubated on ice for 30 minutes. Lysates of 4 wells per condition

were pooled, sonicated on ice, and centrifuged at 16.100 *g* for 20 minutes to remove nuclear debris. A fraction of the supernatant was saved as an input sample, whereas the remaining fraction was incubated overnight at 4 °C with pre-equilibrated mouse monoclonal M2 anti-Flag beads. After 3 washes with IP buffer, Flag-MCT8 protein complexes were eluted using the M2 Flag peptide (Sigma-Aldrich) in IP buffer according to the manufacturer's protocol. IP eluate and input lysate (20 µL each) were subjected to immunoblotting as described in the following section.

F. Immunoblotting

For immunoblots on total cell lysates, JEG-3 and COS-1 cells were cultured in 6-well plates and transfected with 500 ng WT or mutant MCT8 (unless indicated otherwise). Two days after transfection, cells were rinsed once with Dulbecco's PBS, collected in a 100 mM sodium phosphate buffer containing 2 mM EDTA (P100E2, pH 7.2), and sonicated on ice. Protein levels were measured using a Bradford assay (BIO-RAD). After heating for 10 minutes at 70 °C in the presence of NuPAGE 1× lithium dodecyl sulfate (LDS) loading buffer (Thermo Scientific) and 10 mM DTT (unless otherwise indicated), 25 µg protein was separated on a 10% or 4% to 15% gradient mini-PROTEAN TGX Precast Protein Gel (BIO-RAD), blotted to polyvinylidene difluoride membranes, and probed as indicated in the figure legends with rabbit anti-MCT8 antiserum (directed against the C-terminus) [22], mouse M2 anti-Flag Ab (RRID: AB_262044 [26]), rabbit anti-Myc Ab (RRID: AB_439680 [27]), rabbit anti-MCT8 Ab (directed against the N-terminus, RRID: AB_1079343 [28]), or MCT10 antiserum [23] (Supplemental Table 1) [19]. Mouse antiglyceraldehyde-3-phosphate dehydrogenase (GAPDH) (RRID: AB_2107445 [29]) and/or mouse anti–ZO-1 Ab (RRID: AB_2533147 [30]) were used as controls in coimmunoprecipitation (co-IP) studies. IRDye680 goat anti-mouse (RRID: AB_10706161 [31]) and IRDye800 goat anti-rabbit (RRID: AB_621843 [32]) Abs 1:20,000 (LI-COR) were used as secondary Abs. Abs were detected with Odyssey Infrared Detection System (LI-COR).

G. Native Polyacrylamide Gel Electrophoresis

For native polyacrylamide gel electrophoresis (PAGE), cells were cultured as described for conventional immunoblotting. Lysates were prepared in P100E2 buffer and sonicated for 10 seconds on ice, and after addition of native sample loading buffer (final concentrations: 31.25 mM Tris-HCl (pH 6.8), 12.5% glycerol, 0.5% bromophenol blue), 25 µg was separated on a 4% to 15% precast mini-PROTEAN TGX gradient gel (BIO-RAD) under native conditions (1× PAGE buffer: 25 mM Tris-base, 192 mM glycine, ~pH 8.3), and further processed as described for conventional immunoblots.

H. Surface Biotinylation Assays

For surface biotinylation assays, cells were cultured on 10-cm dishes and transfected with 2000 ng of the indicated constructs at 75% confluence. Two days after transfection, surface proteins were labeled with sulfo-NHS-biotin (Thermo Scientific) and isolated according to previously described methods [6].

I. Immunocytochemistry

JEG3 cells were cultured on 10-mm glass coverslips coated with poly-D-lysine (Sigma-Aldrich) and transfected with 250 ng WT or mutant MCT8. After 24 hours, the cells were fixed with 4% paraformaldehyde for 20 minutes at 37 °C, permeabilized with 0.2% triton X-100 (Sigma-Aldrich) in PBS for 5 minutes at room temperature. Samples were blocked for 1 hour at room temperature in PBS containing 2% bovine serum albumin and incubated overnight with N-terminal MCT8 Ab 3353 (1:1000, Sigma-Aldrich), or C-terminal MCT8 antiserum

(1:500) and mouse monoclonal ZO-1 Ab (1:500, Invitrogen) at 4 °C (Supplemental Table 1) [19]. After secondary staining with goat-antirabbit Alexa Fluor 488 (RRID:AB_143165 [33]) and goat-antimouse Alexa 633 (RRID: AB_2535718 [34]) (Invitrogen), cover slips were mounted on glass slides with Prolong Gold containing DAPI (4′,6-diamidino-2-phenylindole) (Invitrogen). Samples were examined on a Zeiss Meta 510 microscope using Zeiss LSM software (Carl Zeiss B.V.).

J. Homology Modeling

YASARA Structure was used for molecular homology modelling of a putative homodimeric MCT8 complex using our previously published MCT8 homology model in outward-open conformation [6, 35-37]. Two MCT8 monomers were manually juxtapositioned in a way that accommodates our in vitro findings. Molecular dynamic simulations were performed in an AMBER 14 force field with periodic boundaries for 4 nanoseconds to establish and optimize the interactions between the 2 monomers, as previously described [6]. All images were created using YASARA Structure and Pov-Ray v3.6 software (www.povray.org).

K. Statistical Analysis

All uptake results are expressed as means ± SEM of at least 3 separate experiments in duplicate. Statistical significance was determined using indicated statistical tests carried out in GraphPad Prism, version 6.

2. Results

In line with previous studies (eg, [7].), MCT8 monomers (55 kDa), homodimers (110 kDa), and putative homo-oligomers (multiples of 55 kDa) were detected on a conventional immunoblot in total lysates of COS-1 cells transiently expressing WT MCT8 after preincubation with LDS sample buffer containing 10 mM DTT (Supplemental Fig. 2A) [19]. To study whether Mg^{2+} and Ca^{2+} mediate these monomer-monomer interactions, lysates were incubated in the presence of increasing concentrations of the Mg^{2+}/Ca^{2+} chelator EDTA prior to immunoblot analysis. However, no reduction in oligomerization was observed (Supplemental Fig. 2A) [19]. Moreover, lysates incubated in the presence of increasing concentrations DTT showed similar levels of oligomerization as those incubated in the absence of DTT, suggesting that disulfide bonds do not play a major role (Supplemental Fig. 2B) [19]. In addition, bands corresponding to the size of WT MCT8 homodimeric complexes were detected in skin fibroblasts, which endogenously express MCT8 (Supplemental Fig. 2C) [19].

Importantly, from conventional immunoblots it cannot be concluded whether monomers result from the disruption of multimeric complexes during the experimental procedure. Moreover, it remains unclear whether the MCT8 dimers and oligomers as detected on conventional immunoblots are formed in a cellular context or during sample preparation because of random protein aggregation. To address these questions, we performed anti-Flag co-IP experiments on lysates of COS-1 cells coexpressing WT Flag-MCT8 and Myc-MCT8 or a mixture of lysates derived from COS-1 cells that separately expressed Flag-MCT8 or Myc-MCT8. Myc-MCT8 was coprecipitated when expressed together with Flag-MCT8, but not in mixed lysates from cells separately expressing Myc-MCT8 or Flag-MCT8 (Fig. 1A). This strongly suggests that a cellular context is indeed required for the formation of monomer-monomer interactions. Interestingly, on coexpression of both constructs, the Myc-MCT8 protein is predominantly present as a monomer in the IP sample, indicating that Flag-MCT8/Myc-MCT8 complexes are at least partially disrupted after preincubation in the presence of LDS sample buffer. Importantly, on coexpression of Flag-MCT8 and MCT10, another T3 transporter that shares a 49% amino acid sequence identity with MCT8, MCT10, was not detected in the IP fraction (Supplemental Fig. 3) [19]. This illustrates the specificity of the MCT8 monomer-monomer interactions. To further validate that MCT8 monomer-monomer interactions may

be mediated by noncovalent interactions, we next separated lysates of COS-1 cells transfected with MCT8 expression construct under native conditions. In the absence of LDS in the loading buffer, a pronounced band that poorly migrated through the gel was observed, whereas in the presence of LDS in the loading buffer, multiple bands were visible (Fig. 1B). These findings confirm that MCT8 dimers/oligomers can be disrupted with LDS.

To identify the domains within MCT8 that are involved in oligomerization, we performed an extensive domain screen by introducing the following premature stop mutations in WT MCT8: R245X, Q335X, S448X, and Q520X (mutations identified in patients with MCT8 deficiency), and E206X, C231X, F256X, C546X (artificial mutations) (Fig. 2A). These constructs are referred to as $MCT8_{75\text{-}244}$, $MCT8_{75\text{-}334}$, $MCT8_{75\text{-}447}$, $MCT8_{75\text{-}519}$, $MCT8_{75\text{-}205}$, $MCT8_{75\text{-}230}$, $MCT8_{75\text{-}255}$, $MCT8_{75\text{-}545}$, respectively. On expression in COS-1 cells, all C-terminal–truncated mutants showed a complete loss of MCT8-mediated TH uptake (Fig. 2B). Similar results were found in JEG-3 cells (data not shown). None of the truncated constructs were expressed at the cell membrane as assessed by confocal microscopy in transiently transfected JEG-3 cells (Fig. 2C). As expected, the monomers of all premature stop mutants were expressed at a molecular weight less than 55 kDa (Fig. 2D). The $MCT8_{75\text{-}334}$, $MCT8_{75\text{-}447}$, $MCT8_{75\text{-}519}$, and $MCT8_{75\text{-}545}$ mutant proteins showed a similar degree of homodimerization as WT MCT8 (Fig. 2E). Similar to WT MCT8, bands at multiples of the molecular weight of the monomer were observed for these mutants, which provides further evidence for the formation of homo-oligomeric complexes. Together, these findings indicate that the C-terminal half of the protein is not required for the stabilization of monomer-monomer interactions. Although the $MCT8_{75\text{-}230}$, $MCT8_{75\text{-}244}$, and $MCT8_{75\text{-}255}$ mutant proteins were still able to form homodimers and homo-oligomers, a relative increase in the monomer fraction was observed (Fig. 2D and 2E). This implies on the one hand that TMD3-6 may contribute to the stabilization of monomer-monomer interactions and on the other hand that a sufficient part of both interaction sites in each monomer is still preserved in the $MCT8_{75\text{-}230}$ mutant protein. Further truncation of the protein completely abrogates homo-oligomerization and severely reduces the stability of homodimeric complexes, as illustrated by the $MCT8_{75\text{-}205}$ mutant (Fig. 2D and 2E). We therefore postulate that the Glu206-Cys231 region (covering part of ECL1 and TMD2) constitutes at least a part of one interaction site, whereas the intracellular N-terminus and/or TMD1 comprise (part of) the second interaction site.

To further explore the role of the intracellular N-terminus in MCT8 oligomerization, a construct lacking all TMDs was generated. Unfortunately, this construct could not be detected at protein level (data not shown). Previous attempts to remove the entire intracellular N-terminal domain (ΔPest) also had detrimental effects on protein expression levels [7]. Therefore, we substituted the intracellular N-terminus of MCT8 by the intracellular N-terminus of MCT1, resulting in an MCT1/8 chimera. As far as we know, the short intracellular N-terminus of MCT1 (9 amino acids long) is not involved in monomer-monomer interactions or interactions with other proteins [38-40]. In addition, N-terminally truncated MCT8 constructs were generated through inactivation of the original translational start site (M75A) and subsequent introduction of 2 downstream alternative start sites (Q97M and R147M , further referred to as $MCT8_{97\text{-}613}$ and $MCT8_{147\text{-}613}$, respectively; Fig. 3A). On transient expression in COS-1 cells, $MCT8_{97\text{-}613}$ showed near-normal TH uptake, whereas TH transport by $MCT8_{147\text{-}613}$ amounted to 55% of WT (Fig. 3B). The MCT1/8 chimera did not induce TH uptake over background. Similar results were obtained in JEG-3 cells (data not shown).

$MCT8_{97\text{-}613}$ and $MCT8_{147\text{-}613}$ were still expressed at the cell membrane, whereas the MCT1/8 chimera showed a predominant intracellular distribution in JEG-3 cells (Fig. 3C). Using antiserum against the C-terminus of MCT8, $MCT8_{97\text{-}613}$, and $MCT8_{147\text{-}613}$ showed similar expression levels as WT on transient expression in COS-1 (Fig. 3D) and JEG-3 cells (data not shown), whereas the expression level of the MCT1/8 chimera was much lower in both cell lines. Nevertheless, all constructs were detected as monomer and homodimer and low levels of homo-oligomers were detected for WT MCT8, $MCT8_{147\text{-}613}$, and the MCT1/8 chimera (Fig. 3D). These findings indicate that the intracellular N-terminus is not strictly required for oligomer formation, although a stabilizing role cannot be excluded.

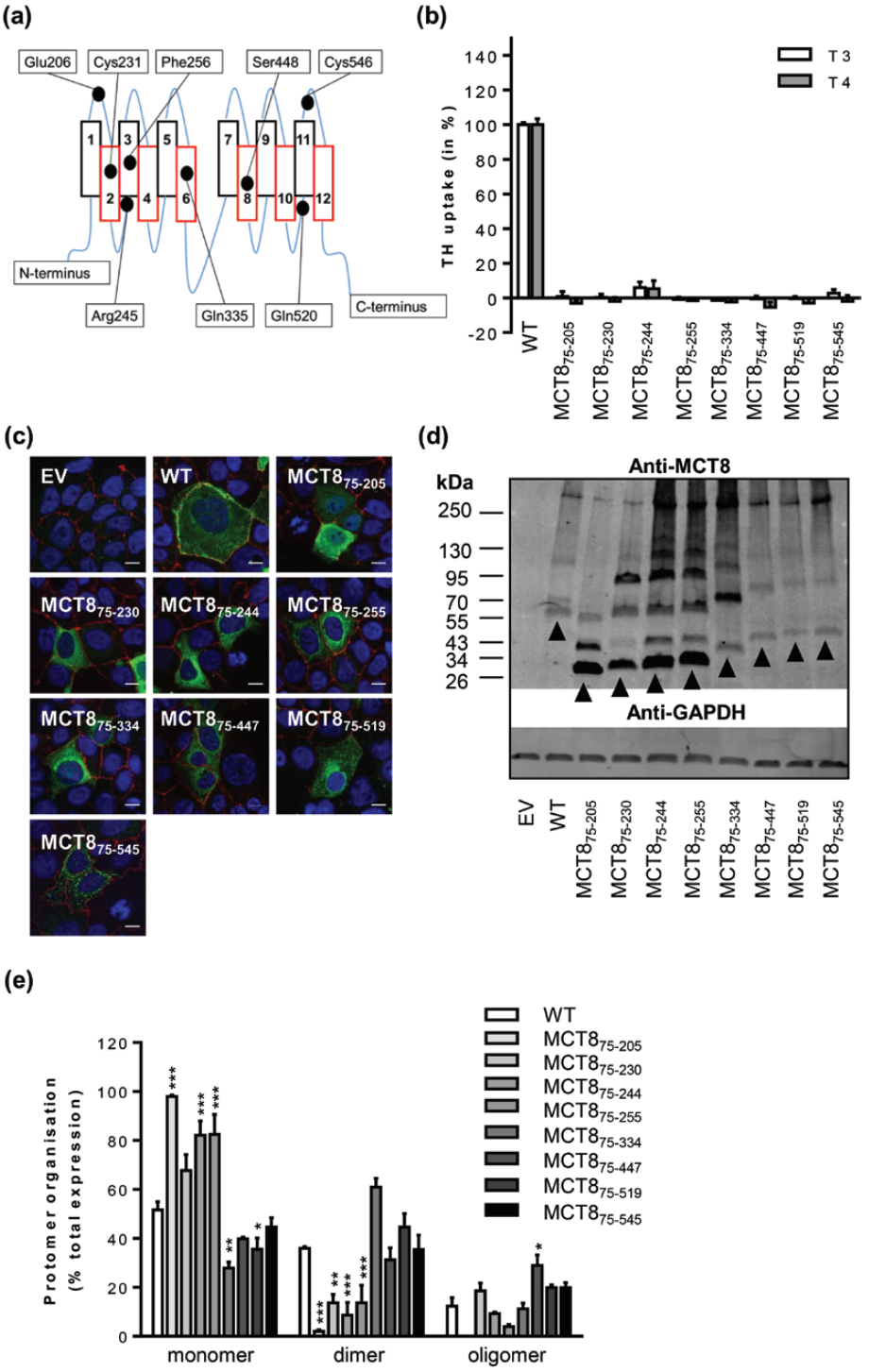

Figure 2. A, Schematic representation of the monocarboxylate transporter 8 (MCT8) protein structure, in which the locations of the C-terminally truncating mutations are indicated. The E206X, C231X, R245X, F256X, Q335X, S448X, Q520X, and C546X mutant proteins will be further referred to as $MCT8_{75\text{-}205}$, $MCT8_{75\text{-}230}$, $MCT8_{75\text{-}244}$, $MCT8_{75\text{-}255}$, $MCT8_{75\text{-}334}$, $MCT8_{75\text{-}447}$, $MCT8_{75\text{-}519}$, $MCT8_{75\text{-}545}$, respectively. B, Uptake of T3 (white bars) and T4 (gray bars) in COS-1 cells transiently transfected with wild-type (WT) MCT8 or the indicated mutant (500 ng) in the presence of human μ-crystallin (250 ng) in 30 minutes at 37 °C. Uptake values are corrected for background thyroid hormone (TH) uptake levels observed in COS-1 cells transfected with pcDNA3 empty vector (EV). Results are presented as means ± SEM (n = 4-7). Statistical significance was tested using 1-way analysis of variance followed by

Interestingly, the M75A construct showed 20% residual TH uptake (Fig. 3B). Several bands were detected for the M75A mutant with the C-terminal antiserum (Fig. 3D), but not using the N-terminal MCT8 Ab (Supplemental Fig. 4) [19]. This suggests the presence of in-frame alternative start-sites (AUG or non-AUG) downstream of residue 155, the end of the recognition sequence of the N-terminal MCT8 Ab. However, on reintroduction of an optimal start site in case of the $MCT8_{97\text{-}613}$ or $MCT8_{147\text{-}613}$ constructs, these bands completely disappeared.

Taken together, these results suggest that both monomer-monomer interaction sites are located within the N-terminal half of the protein. Because the $MCT8_{75\text{-}230}$ mutant protein retained oligomerization potency and the intracellular N-terminus is not essential for oligomer formation, we postulate that one interaction site at least includes TMD1 (Arg147-Glu206) and the other site at least part of ECL1 and TMD2 (Glu206-Cys231). In addition, other domains within the N-terminal half of the protein may also be of importance in stabilization of monomer interactions, which is indeed supported by the observation that the MCT8 construct lacking TMD1 and TMD2 ($MCT8_{\Delta170\text{-}234}$) is still able to form homodimers, homo-oligomers and heterodimeric complexes with WT Flag-MCT8 (Fig. 4A). As expected, the $MCT8_{\Delta170\text{-}234}$ protein is functionally inactive (Fig. 4B) and not expressed at the cell membrane (Fig. 4C).

Next, we aimed to incorporate these in vitro findings into a structural model of the MCT8 dimer using our recently published MCT8 homology model in outward-open conformation [6]. Indeed, TMD1 and TMD2 form part of the external surface of the protein and could thus be involved in the formation of monomer-monomer interactions (Fig. 5A,B). The N-terminal halves of 2 MCT8 monomers were juxtapositioned in an orientation that at least allowed the formation of interactions between TMD1 of one monomer and TMD2 of the other (Fig. 5C). On molecular dynamic simulations, extensive contacts were observed between TMD1, TMD5, and TMD6 of one monomer, and TMD2 and TMD4 of the other (Fig. 5C). In line with our in vitro findings, most of the residues involved in these contacts are hydrophobic or charged (Fig. 5D). Although the predictability of the exact structural orientation of intracellular and extracellular loops as well as the C- and N-terminal ends, is generally low in homology models, it is not excluded that also these domains contribute to the formation of monomer-monomer contacts. Importantly, in the current configuration, movement of the C-terminal half of the MCT8 protein is not influenced by MCT8 monomer-monomer interactions. Assuming a rocker switch model for substrate translocation [41], the current structural organization would therefore allow each MCT8 protein to change its conformational status independently of the interacting MCT8 protein(s).

To further confirm this hypothesis, we next aimed to interfere with the formation of MCT8 oligomeric complexes. Given the extensive nature of the interactions between MCT8 monomers, we were unable to generate an MCT8 construct lacking oligomerization potency

---

the Dunnett multiple-comparison test. TH uptake levels for all mutants were significantly lower than WT ($P < .001$). C, Subcellular localization of WT and mutant MCT8 in transiently transfected JEG-3 cells assessed by confocal microscopy. Depicted is the merged image of the nuclear staining with DAPI (4′,6-diamidino-2-phenylindole) (blue), MCT8 staining with goat-antirabbit Alexa488 (green), and ZO-1 staining as a cell membrane marker using goat-antimouse Alexa633 (red). None of the mutants was expressed at the cell membrane. All images were generated using ImageJ software. The scale bar represents 4 μm. D, Representative immunoblot of lysates from COS-1 cells transfected with WT or mutant MCT8 (N = 3). MCT8 detection was performed with the N-terminal MCT8 antibody (3353) and visualized with IRDye680 goat-antirabbit secondary antibody. Glyceraldehyde-3-phosphate dehydrogenase (GAPDH) was used as loading control. Monomers of WT and mutant MCT8 are indicated with arrowheads. E, Quantification of the band intensities for monomer, homodimeric, and oligomeric WT or mutant MCT8 as shown in D by densitometry using ImageJ. The order of the various mutant constructs as listed in the in-figure legend correspondent to the order of the bars. Results are presented as means ± SEM (n = 3). Statistical differences were assessed using a 2-way analysis of variance followed by Dunnett post hoc tests; *P less than .05; **P less than .01; ***P less than .001.

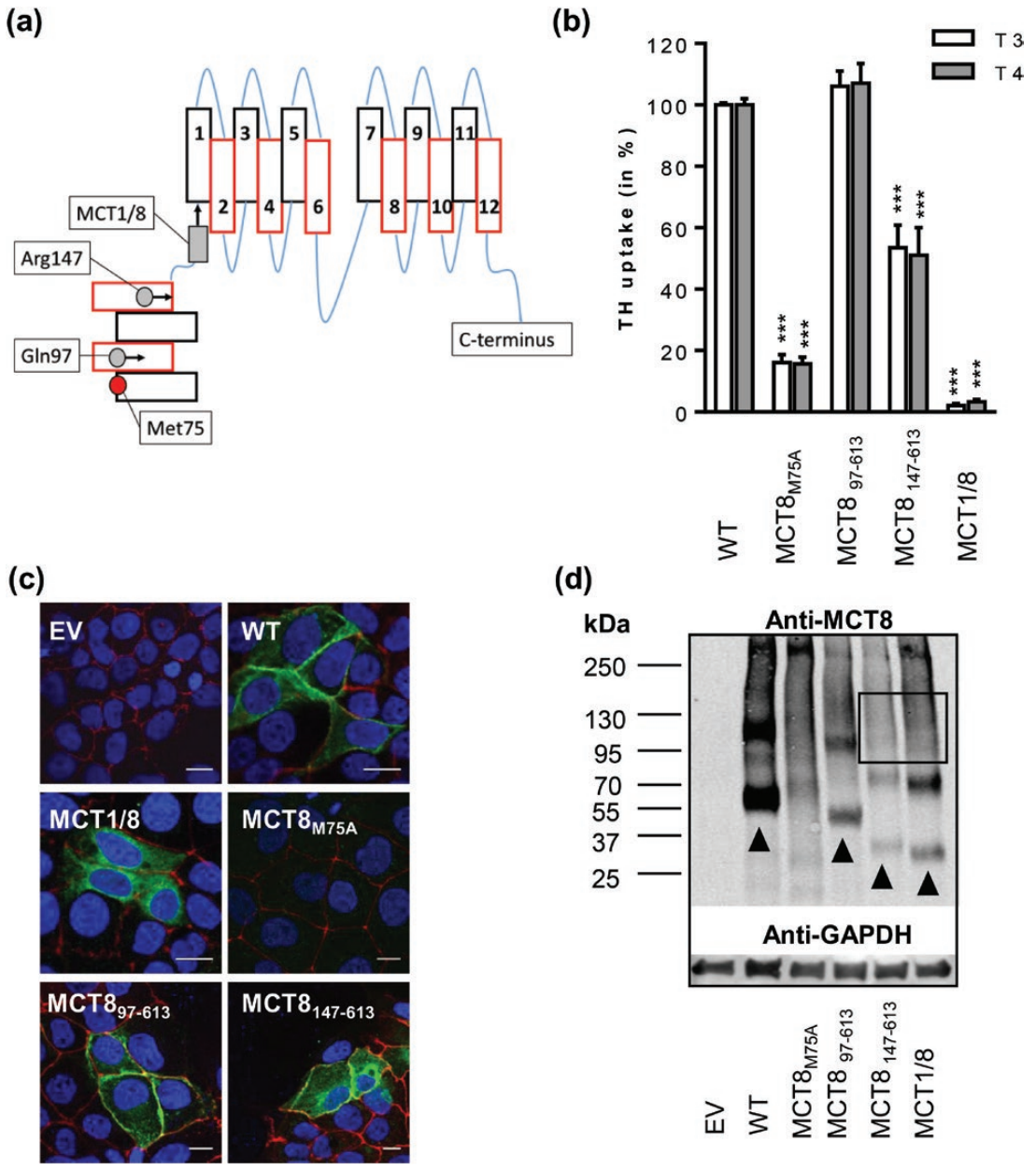

Figure 3. A, Schematic representation of the monocarboxylate transporter 8 (MCT8) protein structure, in which the locations of the N-terminally truncating mutations are indicated. The inactivated original start (Met75) is indicated with a red circle and the introduced translation start sites with gray circles. The gray square represents the short intracellular N-terminus of MCT1 that directly precedes transmembrane domain 1 in the MCT1/8 chimera. B, T3 (white) and T4 (gray) uptake in COS-1 cells transiently transfected with 500 ng wild-type (WT) or mutant MCT8 and 250 ng human μ-crystallin after 30 minutes incubation at 37 °C. Uptake values are corrected for background thyroid hormone (TH) uptake levels observed in COS-1 cells transfected with pcDNA3 empty vector (EV). Results are presented as means ± SEM (n = 3-4). Statistical significance was tested using 1-way analysis of variance followed by the Dunnett multiple-comparison test. ****P* less than .001. C, Subcellular localization of WT and mutant MCT8 in transiently transfected JEG-3 cells assessed by confocal microscopy depicted as described in Fig. 2C. D, Representative immunoblot of lysates from COS-1 cells transfected with WT or indicated mutant MCT8 (n = 3). MCT8 detection was performed with the rabbit anti-MCT8 antiserum (1306, directed against the C-terminus of MCT8) and visualized with IRDye680 goat-antirabbit secondary antibody. Glyceraldehyde-3-phosphate dehydrogenase (GAPDH) was used as loading control. Monomers of WT and mutant MCT8 are indicated with arrowheads. The black box indicates the bands representing oligomers of $MCT8_{147-613}$ and MCT1/8 chimera.

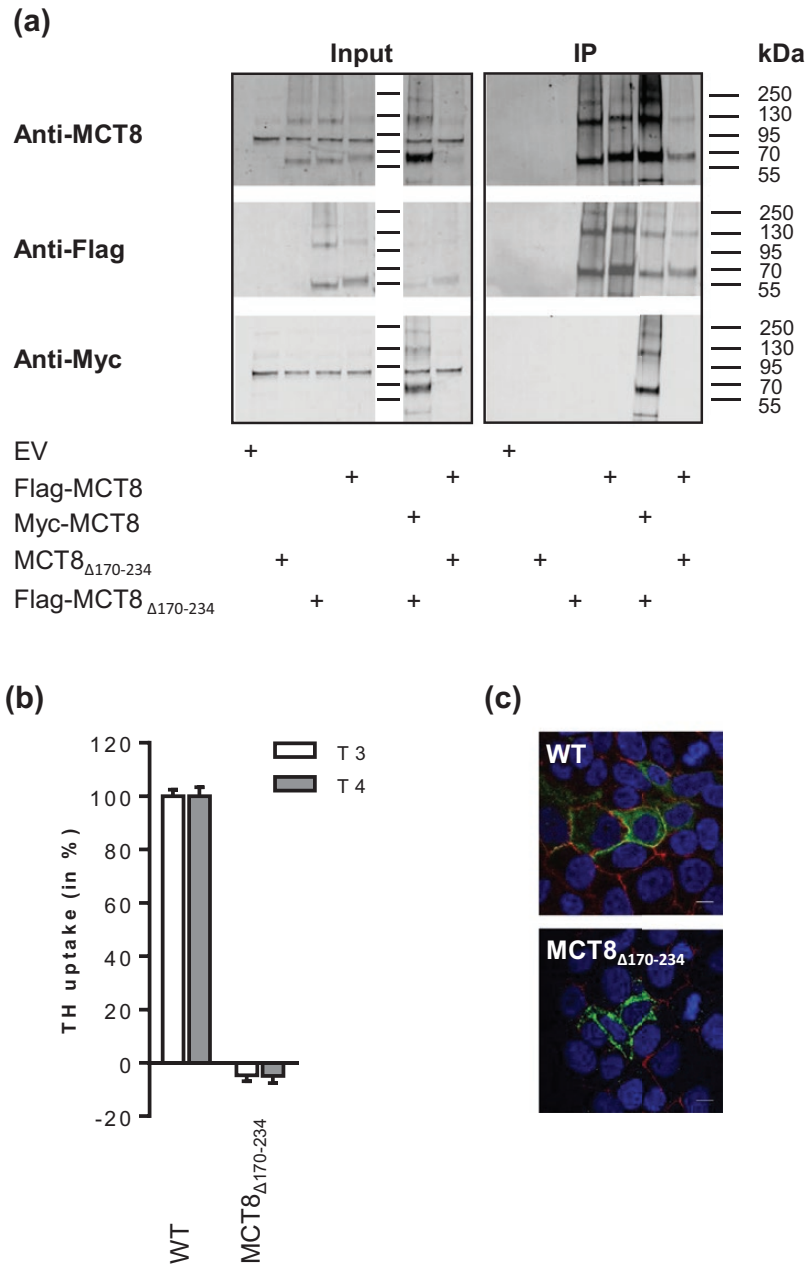

Figure 4. A, Coimmunoprecipitation (co-IP) studies in COS-1 cells (co)expressing wild-type (WT) monocarboxylate transporter 8 (MCT8) or $MCT8_{\Delta 170\text{-}234}$ mutant constructs containing indicated tags (representative blot of 2 repetitive experiments). Membranes have been stained with the mouse monoclonal M2 anti-Flag antibody and rabbit monoclonal anti-Myc, stripped, and subsequently stained with rabbit anti-MCT8 3353 antibody. On coexpression of flag-$MCT8_{\Delta 170\text{-}234}$ and myc-$MCT8_{WT}$, myc-$MCT8_{WT}$ was detected in the precipitated fraction after flag-based co-IPs, indicating that flag-$MCT8_{\Delta 170\text{–}234}$ and myc-$MCT8_{WT}$ form heterodimers. B, T3 (white) and T4 (gray) uptake in COS-1 cells transiently transfected with 500 ng WT MCT8 or the $MCT8_{\Delta 170\text{-}234}$ mutant and 250 ng human μ-crystallin in 30 minutes at 37°C. Uptake values are corrected for background thyroid hormone uptake levels observed in COS-1 cells transfected with pcDNA3 empty vector (EV). Results are presented as means ± SEM (n = 3). Statistical significance was tested using 1-way analysis of variance followed by the Dunnett multiple-comparison test and revealed that T3 and T4 uptake both were significantly reduced in the $MCT8_{\Delta 170\text{-}234}$ mutant ($P < .001$). C, Subcellular localization of WT and mutant MCT8 in transiently transfected JEG-3 cells assessed by confocal microscopy, depicted as described in Fig. 2C.

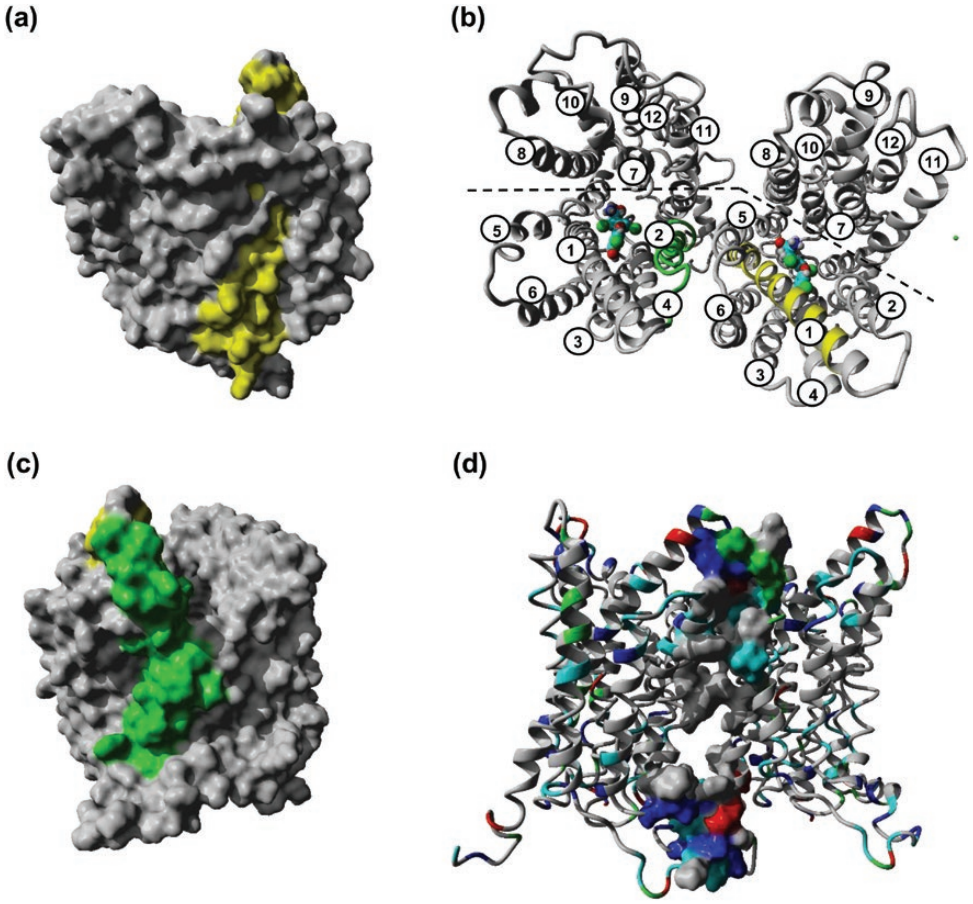

Figure 5. Structural homology model of the monocarboxylate transporter 8 (MCT8) monomer in which A, transmembrane domain 1 (TMD1) and B, transmembrane domain 2 (TMD2) are highlighted in yellow and green, respectively. Parts of both TMDs compose the outer surface of the MCT8 protein. C, A putative organization of an MCT8 homodimeric complex, allowing the interaction of 2 distinct parts of the N-terminal half of 2 MCT8 proteins. This structural organization allows the formation of oligomeric complexes in which all monomers are interacting via a similar mechanism. Of note, in this orientation the movement of the C-terminal half of the MCT8 protein is not influenced by MCT8 monomer-monomer interactions. Assuming a rocker switch model for substrate translocation, each monomer can change its conformational status independently of the interacting monomer(s). D, Frontal view of C in which the molecular surface is shown of the residues located within 0.5 nM (Ångstrom) from the other MCT8 protein, which theoretically allows interactions. Residues are colored according to residue type: in blue, positively charged residues (Arg, Lys, His); in red, negatively charged residues (Asp, Glu); in gray, hydrophobic residues; in light blue, polar residues containing a hydroxyl group (Ser, Thr, Tyr) and Cys residues; and in green, polar residues with an amide group (Asn, Gln). Note that the majority of MCT8 protein-protein interactions have a hydrophobic or electrostatic nature, which is in line with our in vitro experiments. Moreover, it is not excluded that the intracellular loops (ICLs) and extracellular loops (ECLs), including the large ICL3 that links TMD6 and TMD7, contribute to the formation of monomer-monomer interactions.

without directly affecting its function as a TH transporter. Alternatively, we therefore explored to what extent heterodimerization between WT and functionally inactive truncated mutant MCT8 proteins could abrogate MCT8 function. For this reason we first studied whether the truncated and full-length MCT8 proteins were able to form heterodimers. Co-IP experiments were performed on COS-1 lysates coexpressing WT Flag-MCT8 and either the $MCT8_{75\text{-}519}$ (the largest truncated protein encountered in a patient with MCT8 deficiency), $MCT8_{75\text{-}205}$ (impaired oligomerization and reduced homodimerization), $MCT8_{75\text{-}230}$, or $MCT8_{75\text{-}244}$ (intact homodimerization and oligomerization) mutant proteins. All truncated

mutants, including $MCT8_{75-205}$, were detected in the IP fraction only if coexpressed with WT Flag-MCT8, (Fig. 6). In addition, bands representing the intact heterodimers of WT MCT8 and the $MCT8_{75-230}$ and $MCT8_{75-244}$ mutants were detected. These findings support the presence of a common dimerization mechanism and moreover suggest that the formation of interactions between WT and mutant MCT8 proteins already takes place before the trafficking to the cell membrane, because none of the truncated mutants is expressed at the cell membrane if expressed individually (Fig. 2C).

Finally, we studied to what extent increasing concentrations of the $MCT8_{75-230}$ mutant could interfere with WT MCT8 TH transport function by competitive interference with WT MCT8 homodimerization/oligomerization. First, we confirmed the absence of the $MCT8_{75-230}$ protein at the plasma membrane in COS-1 cells using surface biotinylation assays (Supplemental Fig. 5) [19]. Next, we performed Flag-tagged mediated co-IP on total lysates of COS-1 cells coexpressing Flag-MCT8 and Myc-MCT8 and increasing amounts of the $MCT8_{75-230}$ mutant. This resulted in a modest reduction of the amount of Myc-MCT8 detected in the IP samples, indicating that $MCT8_{75-230}$ is able to competitively interfere with the formation of WT Flag-MCT8 and Myc-MCT8 interactions (Supplemental Fig. 6A and 6B) [19]. Nevertheless, even in presence of the highest concentration of the $MCT8_{75-230}$ mutant, Myc-MCT8 was still detected in the IP fraction, indicating incomplete disruption of the WT homodimers/oligomers. Parallel uptake assays showed no reduction in T3 uptake levels under these conditions (Supplemental Fig. 6C) [19]. These findings suggest that the observed reduction in homodimer formation does not result in a decrease in TH transport.

3. Discussion

The present study provides novel insights into the mechanism of MCT8 oligomerization. Our findings suggest that MCT8 monomer-monomer interactions are formed through extensive noncovalent interactions between the N-terminal halves of MCT8 monomers, which are likely to be formed early in the trafficking process. Given the extensive nature of these interactions, monomer-monomer interactions could not completely be abolished by targeted

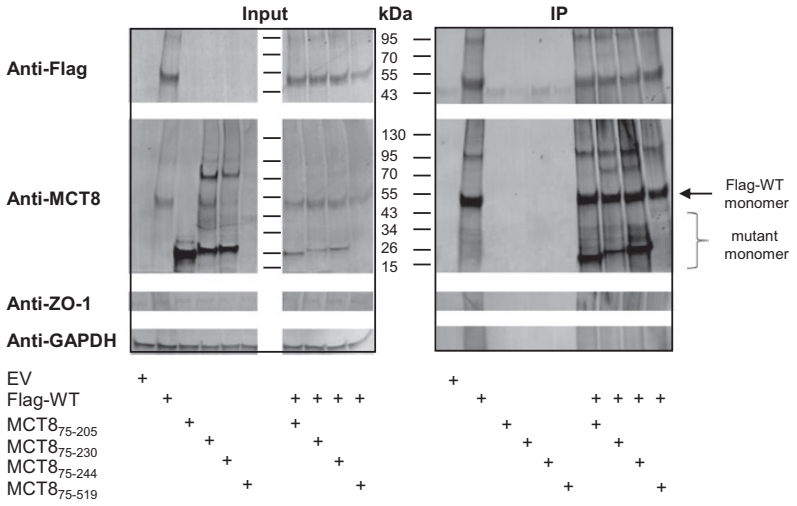

Figure 6. Coimmunoprecipitation (co-IP) studies on lysates derived from COS-1 cells transiently expressing either Flag-MCT8 or indicated mutant monocarboxylate transporter 8 (MCT8) or a combination of Flag-MCT8 and indicated mutant MCT8 constructs. Input and IP samples were run on separate gels (boxed). Blots were stained with rabbit anti-MCT8 antibody and mouse M2 anti-Flag antibody, stripped and stained for mouse anti–ZO-1 (a membrane marker to exclude impurities in the co-IP procedure) and mouse antiglyceraldehyde-3-phosphate dehydrogenase (GAPDH) as loading control. Note the presence of all truncated mutants (bracket) in the IP samples on coexpression with wild-type Flag-MCT8 (arrow), indicating the presence of heterodimers. EV, empty vector

mutations, including large deletions, preventing detailed studies into the physiological function of homodimerization and oligomerization.

Although homodimeric and homo-oligomeric organization of MCT8 has been described in many studies, it has long been unknown whether these complexes are formed inside the cell (eg, [7, 8]). Recent bimolecular fluorescent complementation studies have demonstrated for the first time that at least MCT8 homodimers are likely to be formed in a cellular context [9]. These findings are further substantiated by our present co-IP data showing that the formation of MCT8 dimers and oligomers as detected on immunoblots is not an assay artifact but requires a cellular context.

In an attempt to elucidate the functional role of MCT8 oligomerization, we first aimed to identify the type of interaction(s) that underlie MCT8 oligomerization and the involved domains. Previous studies excluded that disulfide bonding mediates MCT8 oligomerization because each Cys residue in MCT8 can be substituted by an Ala without affecting its oligomerization [17]. Moreover, MCT8 oligomerization was barely enhanced by the Cys cross-linker $HgCl_2$ [7]. Here, we extended on these studies by showing that the addition of increasing concentrations DTT did not affect oligomerization. We also excluded the presence of Ca^{2+}- and Mg^{2+}-mediated oligomerization. Although previous conventional immunoblot studies suggested that MCT8 monomer-monomer interactions could not be completely abrogated by heat and SDS [7], our present co-IP experiments show that a substantial part of the MCT8 dimers are disrupted using LDS sample buffer, even in the absence of DTT. These findings were further substantiated by native PAGE experiments that showed that the addition of LDS is critical to disrupting the MCT8 complexes. Together, these observations have several important implications. First, MCT8 is likely to be predominantly present as a complex under native conditions. Second, disruption of MCT8-MCT8 interactions by LDS suggests that noncovalent interactions (hydrophobic and electrostatic) are involved in MCT8 oligomerization. Finally, at least part of the monomers (and dimers) observed on immunoblots of total lysates are the result of the disruption of MCT8 oligomers during the procedure and thus do not necessarily reflect the amount of monomer inside the cell. It has been previously demonstrated for other proteins that strong hydrophobic interactions can be relatively heat and SDS (and LDS) resistant, which may explain why earlier studies concluded that MCT8 dimerization was SDS resistant [42].

Our successive C-terminal and N-terminal truncation experiments mapped the monomer-monomer interaction sites to the N-terminal half of the MCT8 protein. This part contains 6 TMDs, typically strongly hydrophobic, flanked by charged residues in the extracellular loops and intracellular loops that allow electrostatic interactions. Although we showed that TMD1 and TMD2 are minimally required to form oligomeric complexes, as demonstrated by the $MCT8_{75\text{-}230}$ mutant, specific deletion of these TMDs resulted in a mutant protein that retained its oligomerization capacity. This suggests the presence of extensive monomer-monomer contacts involving other domains beyond TMD1 and TMD2. This was indeed further illustrated by structural modeling of a putative homodimeric conformation of MCT8, which suggested not only the involvement of multiple TMDs, but possibly also loop regions, including the large intracellular loop between TMD6 and TMD7. Of note, removal of a substantial part of the N-terminal PEST-domain (residues 75-147) resulted in a mutant MCT8 protein with substantial residual TH transport capacity, implying that naturally occurring variations in this region are likely to be well tolerated.

In light of our present findings, it is not surprising that although the effects of many missense mutations have been studied, none of these mutations have been found to completely abrogate MCT8 protein-protein interactions (ie, [8, 9, 17, 24]). Nevertheless, a subset of MCT8 missense mutations has been recently described to reduce MCT8 dimerization (S194F, A224T, L434W, and R445C), whereas others were found to enhance dimerization (del230F, V235M, and ins236V) [9]. Because the affected residues in the first group are predicted to be located within the substrate pore, the authors speculated that oligomerization was affected through the effects of these mutations on the overall protein structure and thus protein surface. Interestingly, the mutations that were found to enhance MCT8 dimerization all affect TMD2,

which may well be consistent with a direct contribution of TMD2 in stabilization of the interaction between MCT8 monomers as is also supported by our present data. However, in the present and previously reported studies we found that even large truncations and domain-specific deletions are not sufficient to completely abrogate MCT8 oligomerization [7]. Therefore, we were unable to generate a mutant MCT8 protein that completely lacks homodimerization and oligomerization capacity while retaining residual transport function. As an alternative, we explored whether coexpression of the truncated and functionally inactive $MCT8_{75\text{-}230}$ mutant interferes with WT MCT8 oligomerization. Although this approach resulted in an apparent reduction of interactions between WT MCT8 proteins, they were not completely abrogated. Moreover, no alterations in MCT8-mediated T3 uptake were observed under these conditions. This could mean that, at least in an overexpression system, a substantial alteration in the monomer:oligomer ratio has very little impact on MCT8 function. However, it is not excluded that the $MCT8_{75\text{-}230}$ mutant is mainly competing with WT homo-oligomerization inside the cell and not at the cell membrane given its impaired plasma membrane trafficking. This would result in the exclusive presence of the fully functional WT oligomers at the plasma membrane. The question of whether MCT8 oligomerization is required to achieve (optimal) transporter function thus remains unaddressed. It should however be noted that from a structural perspective, an MCT8 monomer should at least be sufficient to form a transporter channel and function as a transporter (eg, [5].).

Although the effects of truncating mutations on the structure of the remaining MCT8 protein are generally unpredictable, we observed that all truncated proteins were still able to form heterodimers with WT MCT8. This finding at least suggests that the interacting domains in the resulting mutants are still being recognized by the WT protein, which may indicate at least some degree of structural preservation. Because none of the C-terminally truncated proteins reach the plasma membrane if expressed individually (Fig. 2C), the presence of WT-mutant interactions, as assessed by co-IP, may suggest that the formation of MCT8 oligomers is likely to be an early event in the maturation and trafficking of the MCT8 protein. These observations further support recent studies of Fischer et al, showing the presence of MCT8 homodimerization in endoplasmatic reticulum-like structures [9].

Given the important role of MCT8 in the blood-brain barrier and neuronal cells [43], it would have been of interest to study MCT8 oligomerization in vascular endothelial or neuronal cell lines because the presence of cell-type specific factors may importantly influence the type and extent of MCT8 protein-protein interactions. However, such experiments were limited by the poor transfection efficacy of these cell lines (data not shown). Nevertheless, we speculate that the domains involved in homo-oligomerization are not likely to differ between cell lines because this is largely determined by the intrinsic properties of the MCT8 protein.

Taken together, our data show that MCT8 oligomerization is mediated through extensive noncovalent interactions involving TMDs and putative loops within the N-terminal half of the protein. Given the extensive nature of these interactions, we speculate that most mutations encountered in patient with MCT8 deficiency will have only minor effects on the oligomeric organization of MCT8. This is important to the field because the property to form dimeric/oligomeric complexes has been specifically studied in many reports on the impact of mutations identified in patients with MCT8 deficiency.

Acknowledgments

We would like to dedicate this manuscript to the memory of Theo Visser, who suddenly passed away during its finalization. He was deeply involved in the design of these studies and interpretation of the results.

We thank Ramona E. van Heerebeek and Selmar Leeuwenburgh for their technical assistance and the Optical Imaging Center (Erasmus MC Rotterdam) for the technical support regarding the confocal imaging studies.

Financial Support: This work was supported by the Netherlands Organisation for Health Research and Development (project number 113303005 to W.E.V.) and by the Sherman Foundation (to W.E.V.).

Additional Information

Correspondence: Stefan Groeneweg, MD, The Rotterdam Thyroid Center & Department of Internal Medicine, Erasmus Medical Center, Room Ee502, Wytemaweg 80, 3015 CN, Rotterdam, the Netherlands. E-mail: s.groeneweg@erasmusmc.nl.

Disclosure Summary: The authors have nothing to disclose.

Data Availability: All data generated or analyzed during this study are included in this published article or in the data repositories listed in References.

References

1. Friesema EC, Ganguly S, Abdalla A, Manning Fox JE, Halestrap AP, Visser TJ. Identification of monocarboxylate transporter 8 as a specific thyroid hormone transporter. *J Biol Chem*. 2003;**278**(41):40128-40135.
2. Friesema EC, Grueters A, Biebermann H, et al. Association between mutations in a thyroid hormone transporter and severe X-linked psychomotor retardation. *Lancet*. 2004;**364**(9443):1435-1437.
3. Dumitrescu AM, Liao XH, Best TB, Brockmann K, Refetoff S. A novel syndrome combining thyroid and neurological abnormalities is associated with mutations in a monocarboxylate transporter gene. *Am J Hum Genet*. 2004;**74**(1):168-175.
4. Groeneweg S, van Geest FS, Peeters RP, Heuer H, Visser WE. Thyroid hormone transporters. *Endocr Rev*. 2020;**41**(2):146-201.
5. Kinne A, Kleinau G, Hoefig CS, et al. Essential molecular determinants for thyroid hormone transport and first structural implications for monocarboxylate transporter 8. *J Biol Chem*. 2010;**285**(36):28054-28063.
6. Groeneweg S, Lima de Souza EC, Meima ME, Peeters RP, Visser WE, Visser TJ. Outward-open model of thyroid hormone transporter monocarboxylate transporter 8 provides novel structural and functional insights. *Endocrinology*. 2017;**158**(10):3292-3306.
7. Visser WE, Philp NJ, van Dijk TB, et al. Evidence for a homodimeric structure of human monocarboxylate transporter 8. *Endocrinology*. 2009;**150**(11):5163-5170.
8. Biebermann H, Ambrugger P, Tarnow P, von Moers A, Schweizer U, Grueters A. Extended clinical phenotype, endocrine investigations and functional studies of a loss-of-function mutation A150V in the thyroid hormone specific transporter MCT8. *Eur J Endocrinol*. 2005;**153**(3):359-366.
9. Fischer J, Kleinau G, Müller A, et al. Modulation of monocarboxylate transporter 8 oligomerization by specific pathogenic mutations. *J Mol Endocrinol*. 2015;**54**(1):39-50.
10. Yang Y, Mo W, Zhang JT. Role of transmembrane segment 5 and extracellular loop 3 in the homodimerization of human ABCC1. *Biochemistry*. 2010;**49**(51):10854-10861.
11. Wei P, Liu X, Hu MH, et al. The dimerization interface of the glycoprotein Ibβ transmembrane domain corresponds to polar residues within a leucine zipper motif. *Protein Sci*. 2011;**20**(11):1814-1823.
12. Salazar G, Falcon-Perez JM, Harrison R, Faundez V. SLC30A3 (ZnT3) oligomerization by dityrosine bonds regulates its subcellular localization and metal transport capacity. *PloS One*. 2009;**4**(6):e5896.
13. Wei W, Lampe L, Park S, et al. Disulfide bonds within the C2 domain of RAGE play key roles in its dimerization and biogenesis. *PloS One*. 2012;**7**(12):e50736.
14. Pace AJ, Gama L, Breitwieser GE. Dimerization of the calcium-sensing receptor occurs within the extracellular domain and is eliminated by Cys –> Ser mutations at Cys101 and Cys236. *J Biol Chem*. 1999;**274**(17):11629-11634.
15. Boyson JE, Erskine R, Whitman MC, et al. Disulfide bond-mediated dimerization of HLA-G on the cell surface. *Proc Natl Acad Sci U S A*. 2002;**99**(25):16180-16185.
16. Dai Y, Walker SA, de Vet E, Cook S, Welch HC, Lockyer PJ. Ca2+-dependent monomer and dimer formation switches CAPRI Protein between Ras GTPase-activating protein (GAP) and RapGAP activities. *J Biol Chem*. 2011;**286**(22):19905-19916.
17. Lima de Souza EC, Groeneweg S, Visser WE, Peeters RP, Visser TJ. Importance of cysteine residues in the thyroid hormone transporter MCT8. *Endocrinology*. 2013;**154**(5):1948–1955.
18. Mol JA, Visser TJ. Synthesis and some properties of sulfate esters and sulfamates of iodothyronines. *Endocrinology*. 1985;**117**(1):1-7.
19. Groeneweg S, Berge A, Lima De Souza EC, Meima ME, Peeters RP, Visser WE. Insights into the mechanism of MCT8 oligomerization. *J Endocr Soc*. 2020. Deposited January 2, 2020. http://hdl.handle.net/1765/123004
20. RRID:AB_2661880, https://scicrunch.org/resolver/AB_2661880
21. RRID:AB_2661879, https://scicrunch.org/resolver/AB_2661879

22. Friesema EC, Kuiper GG, Jansen J, Visser TJ, Kester MH. Thyroid hormone transport by the human monocarboxylate transporter 8 and its rate-limiting role in intracellular metabolism. *Mol Endocrinol*. 2006;**20**(11):2761-2772.
23. Friesema EC, Jansen J, Jachtenberg JW, Visser WE, Kester MH, Visser TJ. Effective cellular uptake and efflux of thyroid hormone by human monocarboxylate transporter 10. *Mol Endocrinol*. 2008;**22**(6):1357-1369.
24. Novara F, Groeneweg S, Freri E, et al. Clinical and molecular characteristics of SLC16A2 (MCT8) mutations in three families with the Allan-Herndon-Dudley syndrome. *Hum Mutat*. 2017;**38**(3):260-264.
25. Jansen J, Friesema EC, Kester MH, et al. Functional analysis of monocarboxylate transporter 8 mutations identified in patients with X-linked psychomotor retardation and elevated serum triiodothyronine. *J Clin Endocrinol Metab*. 2007;**92**(6):2378-2381.
26. RRID:AB_262044, https://scicrunch.org/resolver/AB_262044.
27. RRID:AB_439680, https://scicrunch.org/resolver/AB_439680.
28. RRID:AB_1079343, https://scicrunch.org/resolver/AB_1079343.
29. RRID:AB_2107445, https://scicrunch.org/resolver/AB_2107445.
30. RRID:AB_2533147, https://scicrunch.org/resolver/AB_2533147.
31. RRID:AB_10706161, https://scicrunch.org/resolver/AB_10706161.
32. RRID:AB_621843, https://scicrunch.org/resolver/AB_621843.
33. RRID:AB_143165, https://scicrunch.org/resolver/AB_143165.
34. RRID:AB_2535718, https://scicrunch.org/resolver/AB_2535718.
35. Krieger E, Vriend G. YASARA View—molecular graphics for all devices—from smartphones to workstations. *Bioinformatics*. 2014;**30**(20):2981-2982.
36. Krieger E, Joo K, Lee J, et al. Improving physical realism, stereochemistry, and side-chain accuracy in homology modeling: four approaches that performed well in CASP8. *Proteins*. 2009;**77**(Suppl 9):114-122.
37. Duan Y, Wu C, Chowdhury S, et al. A point-charge force field for molecular mechanics simulations of proteins based on condensed-phase quantum mechanical calculations. *J Comput Chem*. 2003;**24**(16):1999-2012.
38. Kirk P, Wilson MC, Heddle C, Brown MH, Barclay AN, Halestrap AP. CD147 is tightly associated with lactate transporters MCT1 and MCT4 and facilitates their cell surface expression. *EMBO J*. 2000;**19**(15):3896-3904
39. Deora AA, Philp N, Hu J, Bok D, Rodriguez-Boulan E. Mechanisms regulating tissue-specific polarity of monocarboxylate transporters and their chaperone CD147 in kidney and retinal epithelia. *Proc Natl Acad Sci U S A*. 2005;**102**(45):16245-16250.
40. Wilson MC, Meredith D, Halestrap AP. Fluorescence resonance energy transfer studies on the interaction between the lactate transporter MCT1 and CD147 provide information on the topology and stoichiometry of the complex in situ. *J Biol Chem*. 2002;**277**(5):3666-3672.
41. Forrest LR, Krämer R, Ziegler C. The structural basis of secondary active transport mechanisms. *Biochim Biophys Acta*. 2011;**1807**(2):167-188.
42. Arumugam M, Ajitkumar P. Heat and SDS insensitive NDK dimers are largely stabilised by hydrophobic interaction to form functional hexamer in *Mycobacterium smegmatis*. *Acta Biochim Pol*. 2013;**60**(2):199-207.
43. Vatine GD, Al-Ahmad A, Barriga BK, et al. Modeling psychomotor retardation using iPSCs from MCT8-deficient patients indicates a prominent role for the blood-brain barrier. *Cell Stem Cell*. 2017;**20**(6):831-843.e5.